ACERP: Vol. 3, No. 2, (Spiring 2017) 31-37

Advanced Ceramics Progress

Research Article

Journal Homepage: www.acerp.ir

Enhancing the Bioactivity of a Calcium Phosphate Glass-Ceramic with Controlled Heat Treatment

M. Jalali-Bazehur[a], N. Hatefi-Kargan[a]*, Y. Hatefi[b]

[a]*Department of Physics, University of Sistan and Baluchestan, Zahedan, Iran.*
[b]*Department of Physics, Imam Hossein University, Tehran, Iran.*

P A P E R I N F O

Paper history:
Received 23 April 2017
Accepted in revised form 03 October 2017

Keywords:
Glass-ceramic
Calcium phosphate
Heat treatment
Bioactive

A B S T R A C T

In this paper, bioactive calcium phosphate glass-ceramic has been synthesized by using a facile method and characterized. The glass-ceramic samples were synthesized through heat treating the parent glass at appropriate temperatures, where different calcium phosphate crystalline phases were grown in the parent glass samples during the heat treatment. The amount of elements and oxides in the parent glass were determined by X-ray fluorescence analysis. Using differential scanning calorimetry method, glass transition temperature of the parent glass, and the temperature range for heat treatments were determined. Several calcium phosphate crystalline phases were identified in the glass-ceramic samples. With the increase of heat treatment temperature from 540 to 560°C, β-$Ca_3(PO_4)_2$ and β-$Ca_2P_2O_7$ crystalline phases became the dominant crystalline phases among the other crystalline phases in the glass-ceramic samples. Bioactivity of the glass-ceramic samples was investigated by immersing the samples in Ringer's solution for 7, 21 and 28 days. By analyzing X-ray diffraction patterns, Fourier Transform Infrared (FTIR) spectra, and Scanning Electron Microscopy (SEM) images of the samples immersed in Ringer's solution, the formation of hydroxyapatite on the samples was confirmed. The results show that the samples with β-$Ca_3(PO_4)_2$ and β-$Ca_2P_2O_7$ crystalline phases are more bioactive than others.

1. INTRODUCTION

Glass-ceramics are materials with partially crystalline and partially glass phases that are synthesized with heat treating the parent glass materials [1, 2]. Nucleation, and crystal growth [3, 4] can be controlled in the parent glass, making the glass-ceramics important materials [5]. One of the most important applications of glass-ceramics is in biological and medical applications. These types of glass-ceramics are called bioactive glass-ceramics [6]. For the first time in 1971, Hench *et al.* synthesized a calcium phosphate containing glass-ceramic, called bioglass, and showed that it forms good chemical bonding with the host bone [7]. Although silica based glass-ceramics have shown good bioactivity in medical applications, especially in orthopedics and dentistry, their long term insoluble property causes them to perform reactions. Therefore, calcium phosphate glass-ceramics with controllable properties such as biodegradability, biocompatibility, digestibility due to solubility in water, and bone conduction are better than silica based glass-ceramics, and have been considered in medicine especially in bone replacement and dentistry [8, 9]. Beneficial properties of calcium phosphate glass-ceramics became more visible when Nery *et al.* [10] used a calcium phosphate glass-ceramic as an implant in a dog internal defect surgery. The study showed that the calcium phosphate glass-ceramic is non-toxic, biocompatible and does not cause changes in the calcium and phosphorus levels of blood.

During the laboratory test to assess the bioactivity of a glass-ceramic sample, due to the reaction of nanocrystals with the test solution, hydroxyapatite layer is formed on the sample. The formation of hydroxyapatite layer on a glass-ceramic sample is a confirmation for its bioactivity, and indicates that material could be used in biological and medical applications. From structural point of view, the hydroxyapatite layers formed on bioactive glass-ceramics are very similar to the hydroxyapatite in bone tissue [11]. The crystalline phases in calcium phosphate glass-ceramics affect their bioactivity. From biomedical applications point of view, the main crystalline phases of these glass-ceramics are beta-tricalcium phosphate (β-$Ca_3(PO_4)_2$, β-TCP), biphasic calcium phosphate (BCP), beta-calcium pyrophosphate (β-$Ca_2P_2O_7$, β-CPP), and hydroxyapatite ($Ca_{10}(PO_4)(OH)_2$, HA) [12].

*Corresponding Author's Email: n.hatefi@phys.usb.ac.ir (N. Hatefi)

These crystalline phases can be synthesized in the parent glass by common methods such as heat treatment, sol-gel, petrurgic, etc; and by selecting a suitable composition for the parent glass [4].
Calcium phosphate glass-ceramics based on P_2O_5-CaO glass system are synthesized by adding other materials as nucleation and modifier factors. These glass-ceramics can be synthesized by mixing appropriate amounts of the oxides of the required elements and then melting them which requires higher temperatures. In this study, we have used chlorides of the required elements. This is a facile and cost effective method which lowers the melting temperature.

2. MATERIALS AND METHODS

2.1. Materials In this research, a nominal parent glass material with 75.5% P_2O_5 - 17.9% CaO - 6.6% Na_2O (wt.%) composition was synthesized by mixing and melting 50% P_2O_5, 30% $CaCl_2$, and 20% NaCl (mol.%) powders. The materials after weighting by a digital scale with an accuracy of 10^{-4} grams, were mixed and the resultant mixture was transferred to an alumina crucible for initial cooking on a heater. In order to melt the mixture completely, it was placed in an electric furnace and the furnace temperature was increased over a period of 3 hours from room temperature to 1200°C, and remained at this temperature for one hour. Although the mixture melts at around 800°C, a higher temperature of 1200°C was selected to make a complete and uniform molten material according to our previous experiences. The molten material was transferred into a granite mold for cooling to room temperature in air, to form the parent glass material. The parent glass was then grinded by ball mill crushing and sieved under two mesh numbers of 325 and 200, to obtain the glass powder with 45-75 microns particle sizes. In order to synthesize glass-ceramic samples, from the glass powder some samples were selected, and heat treated at 540, 550 and 560°C for 4 hours. These temperatures were chosen because they are within the nucleation and crystal growth temperatures range of the parent glass, determined by using DSC analysis data, as will be discussed later in Section 3.2. It was impossible to go to higher temperatures because at higher temperatures, the samples are attached firmly to substrate, making them useless. For performing the heat treatments, samples were placed inside a cylindrical furnace and the furnace temperature was increased at a rate of 10°C/min to reach the desired temperature.

2.2. Bioactivity test Bioactivity of the samples, i.e. the formation of apatite layer on them, was evaluated by immersing them in Ringer's solution. For this purpose, 2.65 g of each sample was immersed separately in 50 ml of Ringer's solution and were placed in an incubator set to 37°C for periods of 7, 21, and 28 days. The solution was renewed every 5 days. The samples, after immersion for the specified periods, were taken out of the solutions and washed with double distilled water by using filter papers. Then for drying, the samples were placed in an oven at 37°C for 24 hours.

2.3. Characterization methods In order to determine the glass transition temperature (Tg) and the temperature range for the crystal growth inside the parent glass, differential scanning calorimetry (DSC) measurements were performed by using Rheometric STA 1500 thermal analyzer where the temperature was increased with a rate of 10°C /min. For determining existing elements and compositions in the parent glass, X-ray fluorescence (XRF) measurements were performed by using Philips PW 1410 spectrometer. Crystalline phases formed in the glass-ceramic samples were determined by analyzing the X-ray diffraction (XRD) patterns, obtained using Bruker D8 Advance diffractometer with Cu-Kα X-ray radiation at 40 kV and 30 mA. Using the XRD data, the sizes of the nanocrystallites (D) were calculated by using Scherer's equation:

$$D = \frac{K\lambda}{\beta Cos(\theta)} \quad (1)$$

where β, θ, λ, and K are peak width at half maximum intensity expressed in radians, location of the peak, the wavelength of the X-ray radiation, and a constant factor that for spherical particles is equal to 0.9, respectively. To investigate the changes in microstructure and morphology of the samples immersed in Ringer's solution, scanning electron microscopy (SEM) images were taken by using KYKY EM3400M scanning electron microscope, where the samples before the analysis were coated with a thin layer of gold. In addition, in order to identify functional groups and molecular bonds in the glass-ceramic samples, before and after immersion in Ringer's solution, and examining the formation of hydroxyapatite layer on the samples immersed in Ringer's solution, transmittance spectra of the samples were obtained by using PerkinElmer C-92264 Fourier transform infrared (FTIR) spectrometer.

3. RESULT AND DISCUSSION

3.1. XRF analysis The amounts of elements and oxides in the parent glass, obtained by using XRF analysis, are reported in Table 1. In this analysis, the oxides and elements other than P_2O_5, CaO, and Na_2O, are likely due to the entrance of impurities to the parent glass from the crucibles and molds used in the melting and forming processes. As the data shows, the weight percent of P_2O_5 and CaO are smaller than the nominal values stated in Section 2.1. This is due to

evaporation and entrance of impurities during melting and forming processes, which lowers the weight percent of nominal materials. However, the weight percent of Na_2O is slightly higher than the nominal value, which could be due to the additional sodium ions impurity in our crucibles and molds. In contrast to the amount of Cl atoms in the initial mixture used for preparing the parent glass, the amount of Cl atoms in the parent glass is significantly lower. This is due to the reduction of Cl atoms by oxygen atoms during melting process.

TABLE 1. Amount of oxides and elements in the parent glass

Oxide	The amount of oxide (wt%)	Chemical element	The amount of element (ppm)
SiO_2	0.35	Cr	16
Al_2O_3	4.30	Zr	33
Na_2O	6.97	Ni	10
MgO	0.00	Cl	29
K_2O	0.00	Zn	18
TiO_2	0.03	Pb	36
MnO	0.01	Rb	20
CaO	14.78	Cu	0
P_2O_5	72.20	V	16
Fe_2O_3	0.43	Y	18
SO_3	0.00	Mo	33
LOI	0.00	Sr	65

3.2. Thermal analysis

As Fig.1 shows, the glass transition temperature (Tg) of the parent glass is about 420°C and softening temperature (Tx), associated to the minimum point before starting of nucleation and crystal growth, is about 535°C. Crystallization of various crystalline phases in the parent glass is an exothermic reaction. As indicated in Fig. 1, crystal growth rate at Tp=586°C reaches its maximum value. In addition, the figure shows the start of melting temperature of crystalline phases at Tm=685°C with an endothermic valley spanned from 685 to 750°C.

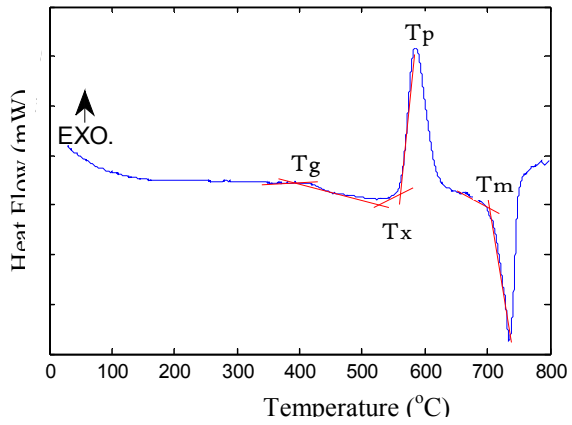

Figure 1. Plot of DSC data measured for the parent glass

3.3. XRD analysis

Fig. 2 shows XRD pattern of the parent glass before applying heat treatment. As the figure shows, the parent glass has amorphous structure. The XRD patterns of the glass-ceramic samples synthesized with heat treating the parent glass samples at 540, 550 and 560°C for 4 hours are shown in Fig. 3. With analyzing the XRD patterns of the glass-ceramic samples, crystalline phases such as tricalcium phosphate ($Ca_3(PO_4)_2$), calcium pyrophosphate ($Ca_2P_2O_7$), sodium calcium phosphate ($NaCa(PO_3)_3$), trisodium phosphate (Na_3PO_4) and calcium metaphosphate (CaP_2O_6) are detected in all samples. The sizes of the nanocrystallites in the the glass-ceramic samples were calculated by using the Scherrer equation. The crystallite size and crystal structure of each type of these nanocrystals have been tabulated in Table 2.

TABLE 2. Crystalline phases determined in the glass-ceramic samples synthesized at 540°C (●), 550°C (□), and 560°C (■)

Crystalline phase	ICDD code	Crystal structure	Crystal size(nm)
$Ca_3(PO_4)_2$	00-003-0960 01-070-2065	Unknow●□ Rhombohedral■	83.34 144.37
$Ca_2P_2O_7$	00-041-0489 00-009-0345 01-071-2123	Monoclinic● Orthorhombic□ Tetragonal■	107.69 65.07 72.94
$NaCa(PO_3)_3$	00-023-0669	Anorthic●□■	86.62
Na_3PO_4	01-076-0202	Tetragonal●□■	55.44
CaP_2O_6	00-015-0204	Unknow●□■	60.26

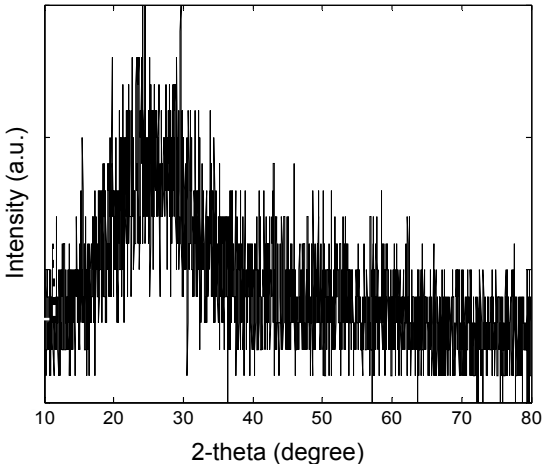

Figure 2. XRD pattern of the parent glass

Fig. 3 shows that with increasing the heat treatment temperature, $Ca_3(PO_4)_2$, $Ca_2P_2O_7$ and $NaCa(PO_3)_3$ crystalline phases have been grown and increased significantly compared with other crystalline phases. As presented in Table 2, $Ca_3(PO_4)_2$ crstalline phase with unknown cystal structure has been formed in the glass-ceramic samples synthesized at 540 and 550°C ; and

$Ca_2P_2O_7$ crystalline phases with monoclinic and orthorhombic cystal structures have been formed in the glass-ceramic samples synthesized at 540 and 550°C, respectively. The dominant crystalline phases in the glass-ceramic samples synthesized at 560°C are β-$Ca3(PO_4)_2$ with rhombohedral crystal structure and β-$Ca_2P_2O_7$ with tetragonal crystal structure.

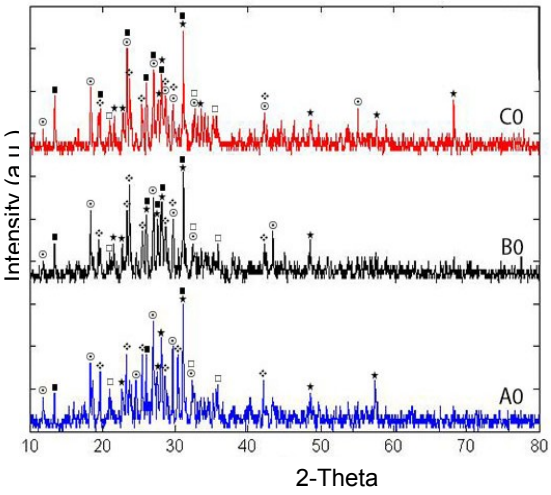

Figure 3. XRD patterns of the glass-ceramic samples synthesized at: 540°C (A0), 550°C (B0), and 560°C (C0). The peaks indicating crystalline phases have been denoted on the figure: $Ca_3(PO_4)_2$ (★), $Ca_2P_2O_7$ (⊙), $NaCa(PO_3)_3$ (■), Na_3PO_4 (□), and CaP_2O_6 (❖)

Fig. 4 shows the XRD patterns of the glass-ceramic samples synthesized at 540°C, before (A0) and after immersion in Ringer's solution for 7 days (A1), 21 days (A2), and 28 days (A3). As the figure shows, there are not characteristic peaks of hydroxyapatite in the XRD pattern of the sample A0 which has not been immersed in Ringer's solution. However, the XRD patterns of immersed samples, especially samples A2 and A3, show characteristic peaks of hydroxyapatite. With the increase of immersion duration, characteristic peaks of hydroxyapatite become more obvious, indicating the growth of hydroxyapatite layer on the samples which were immersed in Ringer's solution.

The XRD patterns of the glass-ceramic samples synthesized at 550 and 560°C, before and after immersion in Ringer's solution, are shown in Figs. 5 and 6. Comparing the XRD patterns of the samples immersed in Ringer's solution, Figs. 4-6, indicate that with the increase in heat treatment temperature from 540 to 560°C the thicknesses of hydroxyapatite layers on the samples increase, while the intensities of the peaks indicating other crystalline phases decrease.

This is due to the reaction of bioactive nanocrystalline phases with Ringer's solution. As Fig. 6 shows, more characteristic peaks of hydroxyapatite phase are apparent in this figure compared with Figs. 4 and 5.

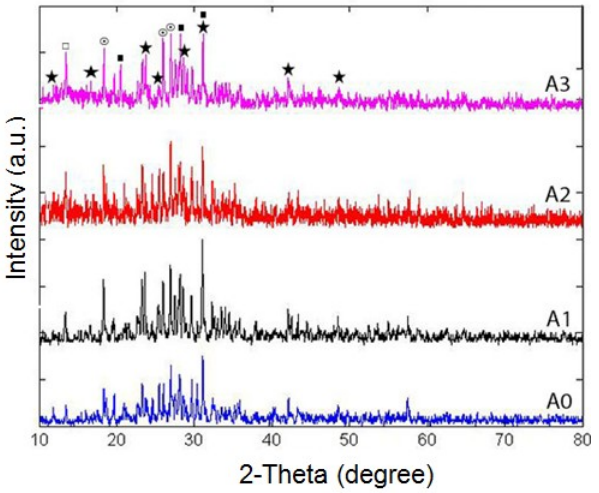

Figure 4. XRD patterns of the glass-ceramic samples synthesized at 540°C: before immersion in Ringer's solution (A0), immersed in Ringer's solution for 7 days (A1), 21 days (A2), and 28 days (A3). The position of characteristic peaks of crystalline phases have been denoted on the figure: $Ca_{10}(PO_4)_6(OH)_2$ (★), $Ca_3(PO_4)_2$ (■), $Ca_2P_2O_7$ (⊙), $NaCa(PO_3)_3$ (□)

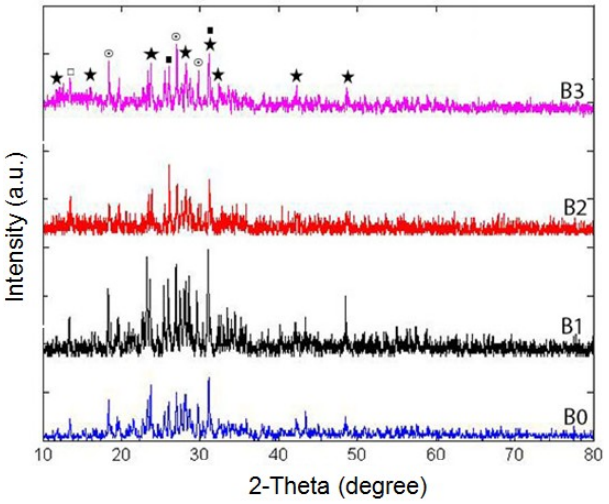

Figure 5. XRD patterns of the glass-ceramic samples synthesized at 550°C: before immersion in Ringer's solution (B0), immersed in Ringer's solution for 7 days (B1), 21 days (B2), and 28 days (B3). The position of characteristic peaks of crystalline phases have been denoted on the figure: $Ca_{10}(PO_4)_6(OH)_2$ (★), $Ca_3(PO_4)_2$ (■), $Ca_2P_2O_7$ (⊙), $NaCa(PO_3)_3$ (□)

This indicates that the thickness of hydroxyapatite layer on the glass-ceramic samples synthesized at 560°C is higher, which shows higher bioactivity of the calcium phosphate glass-ceramic samples synthesized at 560°C compared with the samples synthesized at lower temperatures. Therefore, β-$Ca_3(PO_4)_2$ and β-$Ca_2P_2O_7$ crystalline phases in the glass-ceramic samples are more bioactive than other crystalline phases because these β-

phases are dominant in the glass-ceramic samples which were synthesized at 560°C. These β-phases lead to more reactions of the glass-ceramic samples synthsized at 560°C with Ringer's solution. Therefore, heat treating at 560°C enhances the bioactivity of the glass-ceramic samples synthesized at 560°C.

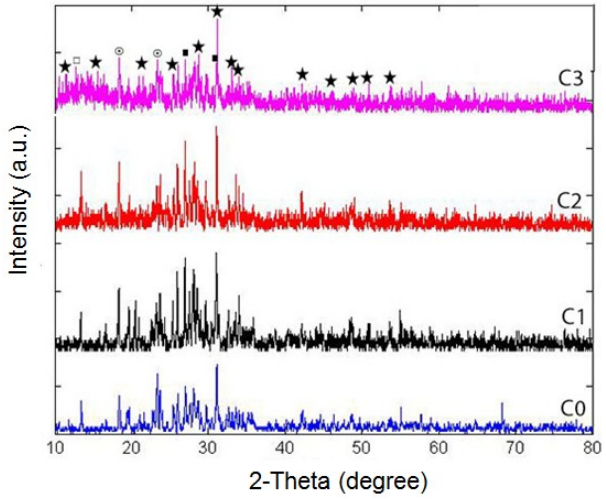

Figure 6. XRD patterns of the glass-ceramic samples synthesized at 560°C: before immersion in Ringer's solution (C0), immersed in Ringer's solution for 7 days (C1), 21 days (C2), and 28 days (C3). The position of characteristic peaks of crystalline phases have been denoted on the figure: $Ca_{10}(PO_4)_6(OH)_2$ (★), $Ca_3(PO_4)_2$ (■), $Ca_2P_2O_7$ (⊙), $NaCa(PO_3)_3$ (□)

3.4. FTIR spectroscopy result

Fig. 7 shows FTIR spectra of the parent glass sample without heat treatment and the glass-ceramic samples synthesized with heat treating the parent glass samples at 540, 550 and 560°C. The absorption peaks at 532-462, 750, 913 and 1300-100 cm^{-1} ranges correspond to the vibration of P-O bonds [13-15]. As Fig. 7 shows, the absorption peaks of the parent glass sample (sample R) are broad, and the absorption peaks at the fingerprint area (1300-900 cm^{-1}) are very weak. However, for the glass-ceramic samples (samples A0, B0, and C0) the mentioned absorption peaks become sharper and stronger. In addition, the FTIR spectra of the glass-ceramic samples at some of the mentioned absorption peaks split into two or more peaks. This is due to formation of the calcium phosphate crystalline phases in glass-ceramics samples. Broad absorption peaks at 1618, 2925 and 3418 cm^{-1} ranges are related to the vibration of O-H linkages, which could be due to water or moisture absorption in the glass-ceramics samples or in KBr pills used for obtaining FTIR spectra [14, 16].

To investigate the bioactivity of the glass-ceramic samples, the absorption peaks of the immersed samples in Ringer's solution are compared with characteristic absorption peaks of hydroxyapatite. Figs. 8-10 show the FTIR spectra of the glass-ceramic samples synthesized at 540, 550 and 560°C and immersed in Ringer's solution for periods of 7, 21 and 28 days.

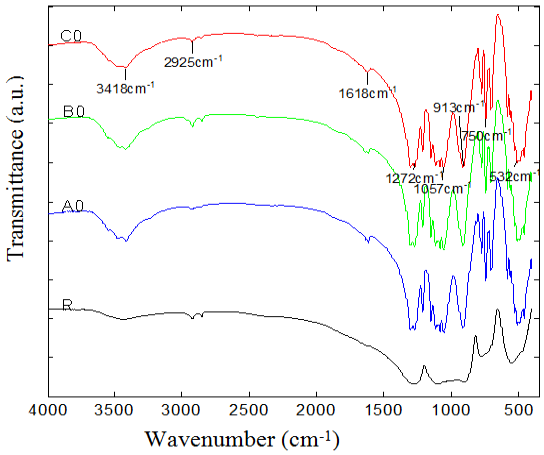

Figure 7. FTIR spectra of the parent glass sample (R) and the glass-ceramic samples synthesized at 540°C (A0), 550°C (B0) and 560°C (C0)

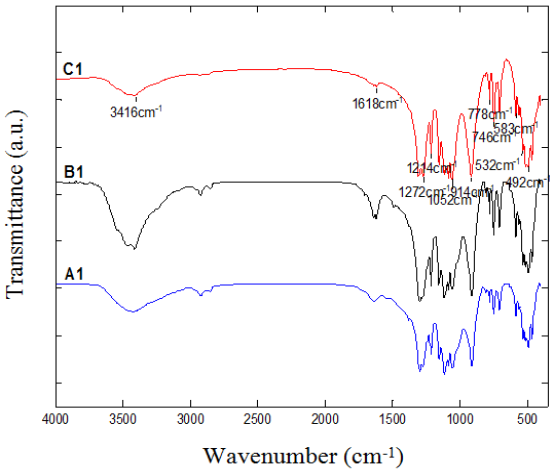

Figure 8. FTIR spectra of the glass-ceramic samples synthesized at 540°C (A1), 550°C (B1), and 560°C (C1); and immersed in Ringer's solution for 7 days

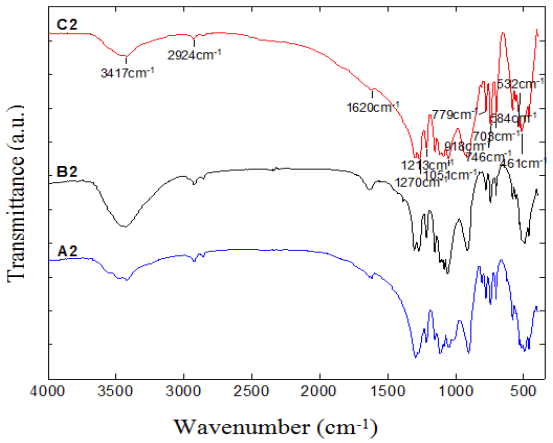

Figure 9. FTIR spectra of the glass-ceramic samples synthesized at 540°C (A2), 550°C (B2), and 560°C (C2); and immersed in Ringer's solution for 21 days.

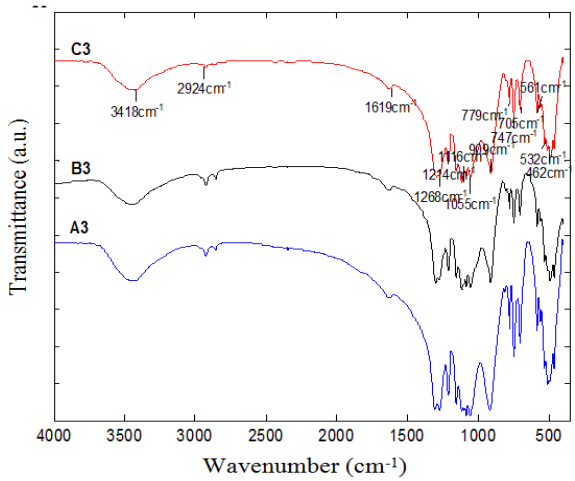

Figure 10. FTIR spectra of the glass-ceramic samples synthesized at: 540°C (A3), 550°C (B3), and 560°C (C3); and immersed in Ringer's solution for 28 days

3.5. SEM images

Figs. 11-13 show SEM images of the glass-ceramic samples synthesized with heat treating the parent glass samples at 540, 550, and 560°C, before and after immersion in Ringer's solution. As the SEM images of the glass-ceramic samples immersed in Ringer's solution show, the morphology of the glass-ceramic samples indicate the growth of hydroxyapatite layer on the samples. The morphologies of the samples synthesized at 560°C and immersed in Ringer's solution are more uniform and have better surface coverage compared with the morphology of other samples, indicating enhanced growth of hydroxyapatite layer on these samples.

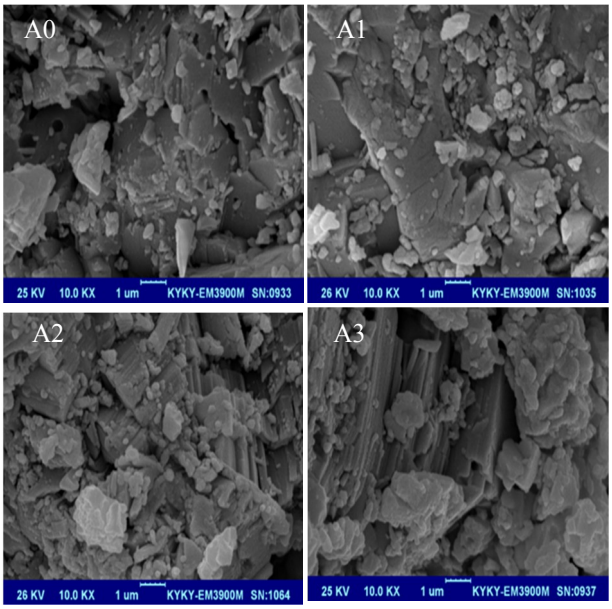

Figure 11. SEM images of the glass-ceramic samples synthesized at 540°C, before immersion in Ringer's solution (A0), and after immersion in Ringer's solution for: 7 days (A1), 21 days (A2), and 28 days (A3)

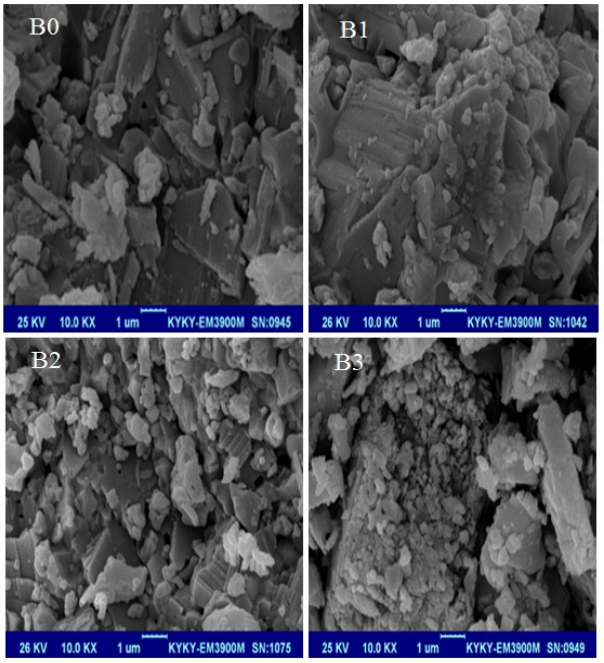

Figure 12. SEM images of the glass-ceramic samples synthesized at 550°C, before immersion in Ringer's solution (B0), and after immersion in Ringer's solution for: 7 days (B1), 21 days (B2), and 28 days (B3)

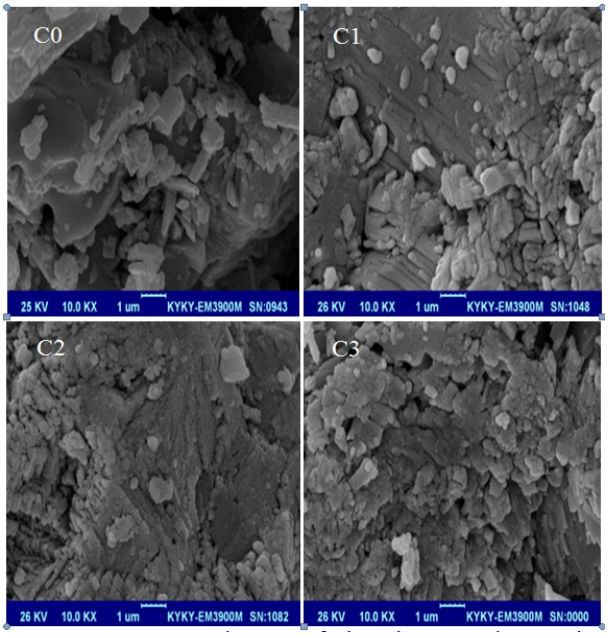

Figure 13. SEM images of the glass-ceramic samples synthesized at 560°C, before immersion in Ringer's solution (C0), and after immersion in Ringer's solution for: 7 days (C1), 21 days (C2), and 28 days (C3).

4. CONCLUSION

In this research, by mixing 50% P_2O_5, 30% $CaCl_2$, and 20% NaCl (in mole percent), and melting them, calcium phosphate glass-ceramic samples were synthesized with

heat treating the parent glass samples at 540, 550, and 560°C. The XRF analysis data indicates that Cl atoms leave the composition during the melting process, and due to the evaporation, the mole fraction of final parent glass is different from the initial powder mixture. The X-ray diffraction patterns, Fourier Transform Infrared (FTIR) spectra, and Scanning Electron Microscopy (SEM) images of the samples show that with heat treating the parent glass at 560°C nanosized crystallites with β-$Ca_3(PO_4)_2$ (rhombohedral) and β-$Ca_2P_2O_7$ (tetragonal) crystalline phases are formed in the parent glass which causes the sample to be more bioactive than the parent glass samples heat treated at other temperatures. This is consistent with the results reported by other researchers about the bioactivity of the β-$Ca_3(PO_4)_2$ and the β-$Ca_2P_2O_7$ crystalline phases.

5-ACKNOWLEDGMENTS

This work was supported by the University of Sistan and Baluchestan.

REFERENCES

1. Marghussian, V., "Nano-Glass Ceramics: Processing, Properties and Applications", Elsevier, Inc.: Oxford, (2015).
2. Höland, W., "Glass-ceramics", in Bio-Glasses: an Introduction, Jones, J.R., Clare, A.G., Eds., John Wiley and Sons, Ltd., Chichester, (2012).
3. Donald, I.W., "Preparation, properties, and chemistry of glass and glass-ceramic-to-metal seals and coating", Journal of Materials Science, Vol. 28, (1993), 2841-2886.
4. Rawlings, R.D., Wu, J.P. and Boccaccini, A.R., "Glass-ceramics: their production from wastes- a review", ***Journal of Materials Science***, Vol. 41, (2006), 733-761.
5. Höland, W. and Beall, G.H., "Glass-Ceramic Technology", 2nd ed., John Wiley and Sons, Inc.: Hoboken, (2012).
6. Kokubo, T., Shigematsu, M., Nagashima, Y., Tashiro, M., Nakamura, T., Yamamuro, T. and Higashi, S., "Apatite- and wollastonite-containing glass-ceramics for prosthetic applications", ***Bulletin of the Institute for Chemical Research***, Vol. 60, (1982), 260-268.
7. Hench, L.L., Splinter, R.J., Allen, W.C. and Greenlee, T.K., "Bonding mechanisms at the interface of ceramic prosthetic materials", ***Journal of Biomedical Materials Research***, Vol. 5, (1971), 117-141.
8. Best, S.M., Porter, A.E., Thian, E.S. and Huang, J., "Bioceramics: past, present and for the future", ***Journal of the European Ceramic Society***, Vol. 28, (2008), 1319-1327.
9. Franks, K., Abrahams, I. and Knowles, J.C., "Development of soluble glasses for biomedical use part I: in vitro solubility measurement", ***Journal of Materials Science: Materials in Medicine***, Vol. 11, (2000), 609-614.
10. Nery, E.B., Lynch, K.L., Hirthe, W.M. and Mueller, K.H., "Bioceramic implants in surgically produced infrabony defects", ***Journal of Periodontology***, Vol. 46, (1975), 328-347.
11. Ha, N.R., Yang, Z.X., Hwang, K.H., Kim, T.S. and Lee, J.K.,. "Improvement of the stability of hydroxyapatite through glass ceramic reinforcement", ***Journal of Nanoscience and Nanotechnology***, Vol. 10, (2010), 3459-3462.
12. Kasuga, T., Terada, M., Nogami, M. and Niinomi, M., "Machinable calcium pyrophosphate glass-ceramics", ***Journal of Materials Research***, Vol. 16, (2001), 876-880.
13. Karmakar, B., "Fundamentals of glass and glass nanocomposites", in Glass Nanocomposites: Synthesis, Properties and Applications, Karmakar, B., Rademann, K., Stepanov, A., Eds., Elsevier Inc., Cambridge, (2016).
14. Pavia, D.L., Lampman, G.M., Kriz, G.S. and Vyvyan, J.R., "Introduction to Spectroscopy", 5th ed., Cengage Learning: Stamford, (2015).
15. Silverstein, R.M., Webster, F.X., Kiemle, D.J. and Bryce, D.L., "Spectrometric Identification of Organic Compounds", 8th ed., John Wiley and Sons, Inc.: Hoboken, (2015).
16. Radev, L., Hristov, V., Michailova, I., Fernandes, M.H.V. and Salvado, I.M.M., "In vitro bioactivity of biphasic calcium phosphate silicate glass-ceramic in CaO-SiO_2-P_2O_5 system", ***Processing and Application of Ceramics***, Vol. 4, (2010), 15-24.
17. Chetty, A.S., Wepener, I., Marei, M.K., Kamary, Y.E. and Moussa, R.M., "Synthesis, properties, and applications of hydroxyapatite", in Hydroxyapatite: Synthesis, Properties and Applications, Gshalaev, V.S., Demirchan, A.C., Eds., Nova Science Publishers, Inc., Hauppauge, (2012).
18. Ooi, C.Y., Hamdi, M. and Ramesh, S., "Properties of hydroxyapatite produced by annealing of bovine bone", ***Ceramics International***, Vol. 33, (2007), 1171-1177.
19. Zhang, Y., Santos, J.D., "Crystallization and microstructure analysis of calcium phosphate-based glass ceramics for biomedical applications", ***Journal of Non-Crystalline Solids***, Vol. 272, (2000), 14-21.
20. Dobradi, A., Enisz-Bodogh, M., Kovacs, K., Korim, T., "Bio-degradation of bioactive glass ceramic containing natural calcium phosphates ", ***Ceramics International***, Vol. 42, (2016), 3706-3714.